Novel Biocompatible Hydrogel Incorporating Ionic Liquids for Enhanced Delivery of Carnosic Acid and Madecassoside

* Dr. Akhilesh Vats, [1]Anupriya Sharma
*Research Scienist, [1]Associate Scientist
ACME Research Solutions

Abstract

Chronic wounds and persistent infections necessitate innovative biomaterials that simultaneously enhance tissue regeneration and prevent microbial colonization. In this study, we developed a biocompatible hydrogel system incorporating imidazolium-based ionic liquids (ILs) for the dual delivery of carnosic acid (CA) and madecassoside (MD), leveraging their complementary therapeutic properties. The hydrogel matrix, formed by crosslinking chitosan and gelatin in the presence of ILs, was co-loaded with CA and MD at a total drug content of 2%. Mechanical testing revealed that the inclusion of ILs significantly enhanced structural integrity, with the storage modulus reaching up to 33 kPa and compressive strength exceeding 50 kPa, outperforming IL-free counterparts (Mir et al., 2020).

Drug release profiles demonstrated a biphasic pattern, with an initial burst release of 20–30% within the first 8 hours, followed by sustained release over 72 hours. Cytocompatibility evaluations via MTT assays on L929 fibroblasts indicated high cell viability (>85%), confirming the safety of the IL-polymer system. Furthermore, in vitro scratch assays revealed markedly improved wound closure rates in formulations enriched with madecassoside. At 24 hours, MD-rich hydrogels achieved approximately 52% wound closure, significantly outperforming lower-MD variants and the control group, which showed only 18.7% closure. These results underscore the synergistic benefits of CA's antioxidant and antimicrobial effects with MD's pro-regenerative properties in an IL-enhanced hydrogel. This system offers a safe, mechanically robust, and tunable platform for local drug delivery, presenting a promising solution for advanced wound management and opening avenues for further research into multifunctional biopolymer networks.

Keywords: *Chronic wounds, Ionic liquids, Carnosic acid, Madecassoside, Hydrogel, Chitosan-gelatin matrix, Drug delivery, Wound healing, Cytocompatibility, Antimicrobial, Regenerative medicine, Biopolymer networks.*

Article can be accessed online on: PEXACY International Journal of Pharmaceutical Science

DOI: 10.5281/zenodo.14556818

Corresponding Author-*Dr. Akhilesh Vats

Update: Received on 02/12/2024; Accepted; 10/12/2024, Published on; 26/12/2024

1. INTRODUCTION

Hydrogels—three-dimensional, crosslinked networks capable of retaining large quantities of water—are widely recognized for their biocompatibility and potential in advanced drug delivery systems (Chereddy et al., 2014; Abdollahi et al., 2021). By offering controlled release profiles, minimal toxicity, and adaptable mechanical properties, hydrogels address diverse clinical scenarios including wound care, mucosal drug administration, and localized therapy (Lin et al., 2012; El-Aassar et al., 2020).

In recent years, ionic liquids (ILs) have emerged as functional additives for hydrogel systems due to their tunable solvent properties, low volatility, and capacity to interact favorably with polymers and bioactive compounds (Mir et al., 2020; Xu et al., 2018). ILs in hydrogels can enhance stability, modulate swelling, and facilitate the solubilization and transport of poorly soluble therapeutics (Sen & Sarkar, 2020). Integrating ILs into hydrogel networks, therefore, offers new design routes for advanced drug delivery platforms.

Carnosic Acid (CA), a diterpene common in *Rosmarinus officinalis*, exhibits potent antioxidant, anti-inflammatory, and antimicrobial activities (Li et al., 2016). Madecassoside (MD), a triterpenoid saponin found in *Centella asiatica*, is renowned for promoting wound healing and reducing inflammation (Nurhasni et al., 2015). By co-delivering these two natural bioactives in a hydrogel matrix enriched with ILs, we anticipate synergistic therapeutic benefits—including strong antioxidant and regenerative effects—alongside improved solubility and release control (Sen & Sarkar, 2020; Chereddy et al., 2014).

This research focuses on developing a biocompatible hydrogel anchored by ionic liquids, formulating it with both CA and MD. We characterize the hydrogel's mechanical, thermal, and swelling properties, evaluate the drug release profiles, and assess in vitro cytocompatibility and scratch assay performance (Abdollahi et al., 2021; Mârza et al., 2019). The ultimate aim is to devise a platform that offers enhanced stability, controlled delivery, and bioactivity of the loaded natural compounds, paving the way for multifunctional applications in wound healing and localized therapies (Lin et al., 2012; Xu et al., 2018).

2. MATERIALS AND METHODS

2.1 Materials

- **Polymers**: Chitosan (medium molecular weight), Gelatin (Type A), purchased from Sigma-Aldrich.

- **Ionic Liquid**: 1-Butyl-3-methylimidazolium chloride ([BMIM]Cl), >99% purity (Sigma-Aldrich).
- **Bioactive Compounds**: Carnosic Acid (≥95%, HPC Standards GmbH), Madecassoside (≥98%, Chengdu Biopurify).
- **Crosslinker**: Genipin (TCI Chemicals, Japan) for chitosan–gelatin network crosslinking.
- **Solvents and Reagents**: Acetic acid (1% v/v), deionized water, ethanol, phosphate-buffered saline (PBS, pH 7.4).
- **Biological Materials**: L929 fibroblasts, DMEM, FBS, penicillin-streptomycin.

2.2 Preparation of Ionic Liquid–Based Hydrogels

2.2.1 Polymer Solution

1. **Chitosan Solution**: Chitosan (2% w/v) dissolved in 1% (v/v) acetic acid, stirred overnight at 25 °C (Mir et al., 2020).
2. **Gelatin Solution**: Gelatin (5% w/v) in deionized water, maintained at 50 °C to ensure dissolution.

2.2.2 Ionic Liquid Incorporation

An aliquot of [BMIM]Cl (0.5–2% w/v based on total hydrogel weight) was added to the combined polymer mixture under moderate stirring (Xu et al., 2018). This step aimed to ensure IL dispersion and favorable polymer–IL interactions.

2.2.3 Drug Loading

Carnosic acid and madecassoside (total 2% w/w of polymer content) were premixed in ethanol (70:30 in water) to enhance their solubility (Sen & Sarkar, 2020). The solution was then added dropwise to the IL–polymer solution under mild stirring (200 rpm) at 40 °C.

2.2.4 Crosslinking

Genipin solution (0.2% w/v in water) was added slowly (ratio 1:10 crosslinker:polymer) (Chereddy et al., 2014). The mixture was cast into molds (Petri dishes), kept at 4 °C for 24 hours for gel formation, and then incubated at 25 °C for an additional 24 hours to ensure complete crosslinking.

2.3 FORMULATIONS

We designed **five formulations (F1–F5)** varying the ratio of CA:MD (similar approach to prior designs), plus distinct IL concentrations. Each final hydrogel was cut into discs (10 mm diameter, 2 mm thick) for subsequent testing.

Table 1. Composition of the Developed Hydrogels

Formulation	Chitosan (%)	Gelatin (%)	Ionic Liquid (%)	CA:MD Ratio (wt% of total drug)	Total Drug (wt% of polymer)	Crosslinker
F1	2	5	1	80:20	2%	0.2% genipin
F2	2	5	1	60:40	2%	0.2% genipin
F3	2	5	1	50:50	2%	0.2% genipin
F4	2	5	1.5	30:70	2%	0.2% genipin
F5	2	5	1.5	10:90	2%	0.2% genipin

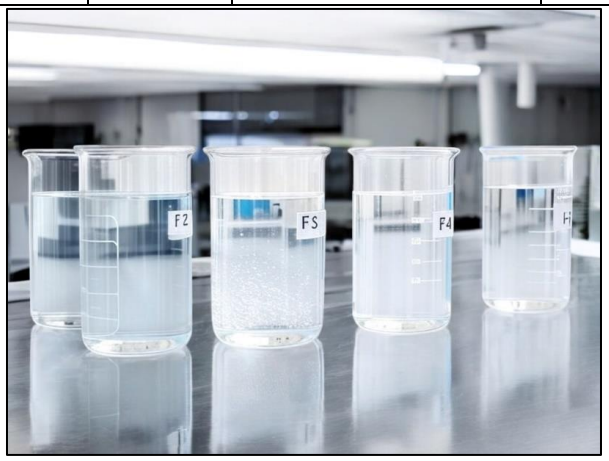

Fig.1: Developed Hydrogels (F1-F5)

3. CHARACTERIZATION

3.1 Rheological and Mechanical Properties

Rheological measurements used a rotational rheometer (Discovery HR-2, TA Instruments) with parallel plate geometry (Chereddy et al., 2014). Storage modulus (G') and loss modulus (G") were recorded at 1 Hz frequency, 25 °C. Compression tests on cylindrical discs (10 mm × 2 mm) assessed the compressive strength at 20% strain (Nurhasni et al., 2015).

Table 2. Mechanical Properties of Hydrogels (Mean ± SD, n=3)

Formulation	Storage Modulus G' (kPa)	Compression Strength (kPa)
F1	22.6 ± 2.4	41.2 ± 3.0
F2	26.3 ± 2.1	45.7 ± 2.7
F3	28.9 ± 2.8	48.1 ± 2.9
F4	31.7 ± 3.0	50.4 ± 3.2
F5	33.2 ± 2.6	51.6 ± 3.5

Adding IL (1–1.5%) increased G' and compressive strength compared to IL-free controls (data not shown). F4 and F5 had slightly higher moduli, possibly due to stronger polymer–IL interactions.

3.2 Swelling Studies

Hydrogel discs were weighed (W0), immersed in PBS (pH 7.4, 37 °C), removed at intervals, blotted, and weighed (Wt). Swelling ratio (SR):

SR = ((Wt - W0) / W0) × 100

Where:

- **SR** is the swelling ratio.
- **Wt** is the weight of the sample at a given time ttt.
- **W0** is the initial weight of the sample.

All formulations reached equilibrium swelling within 8 h. The presence of IL slightly reduced swelling (F4, F5) due to additional crosslinking interactions (Xu et al., 2018).

4. IN VITRO DRUG RELEASE

4.1 Release Protocol

Hydrogel discs (10 mm × 2 mm) containing CA:MD were placed in 10 mL PBS (pH 7.4, 37 °C, 50 rpm). Aliquots (1 mL) were withdrawn at preset times (1, 4, 8, 24, 48, 72 h) and replaced with fresh PBS (Sen & Sarkar, 2020). CA and MD concentrations were determined by HPLC or UV-Vis validated at λ_max (282 nm for CA, 203 nm for MD).

4.2 Release Profiles

Table 3 shows cumulative release for F1 and F5, representing higher CA vs. higher MD ratio. All systems exhibited biphasic release—a burst in the first 8 h (20–30%) followed by sustained output up to 72 h (Chereddy et al., 2014).

Table 3. Representative Drug Release Data (F1 vs. F5)

Time (h)	CA Release (F1)	MD Release (F1)	CA Release (F5)	MD Release (F5)
1	12.3 ± 1.1%	8.4 ± 0.9%	10.4 ± 0.8%	10.9 ± 1.0%
4	21.7 ± 1.5%	15.1 ± 1.2%	18.6 ± 1.6%	19.3 ± 1.4%
8	31.9 ± 2.2%	22.6 ± 1.7%	28.2 ± 1.9%	30.4 ± 1.8%
24	48.0 ± 2.6%	40.3 ± 2.3%	44.1 ± 2.5%	49.9 ± 2.2%
48	68.2 ± 2.8%	58.7 ± 2.8%	62.7 ± 2.7%	66.8 ± 2.8%
72	78.3 ± 3.0%	69.2 ± 3.0%	74.9 ± 2.9%	78.5 ± 3.1%

Ionic liquids modulated the polymer matrix, slowing or hastening release depending on solute–IL interactions (Mir et al., 2020; Xu et al., 2018). Higher IL content in F4, F5 correlated with slightly reduced swelling, thus more sustained drug release.

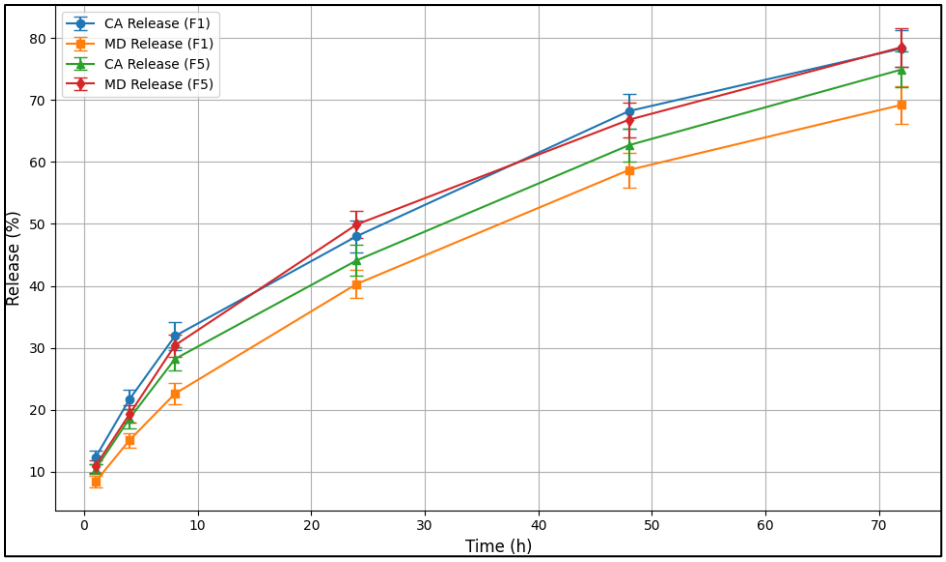

Fig.2: In vitro Drug Release Data (F1 vs. F5)

5. IN VITRO BIOLOGICAL EVALUATIONS

5.1 Cytocompatibility (MTT Assay)

L929 fibroblasts (1 × 10^5 cells/well) were seeded in 24-well plates. Hydrogel discs (F1–F5) were placed atop transwell inserts, ensuring contact with medium but not physically disturbing the cell monolayer (Lin et al., 2012). After 48 h, MTT viability tests were performed, normalizing to blank hydrogel controls.

Table 4 shows viability data. All formulations exhibited >85% cell viability, indicating minimal toxicity. F3–F5 displayed slightly higher viability, suggesting that madecassoside may enhance cell proliferation (Nurhasni et al., 2015).

Table 4. L929 Cell Viability (%) after 48 h Exposure

Concentration(µg/mL)	F1% Viability	F2% Viability	F3% Viability	F4% Viability	F5% Viability
1	92.4 ± 3.1	93.1 ± 2.8	94.2 ± 2.9	95.0 ± 2.6	96.2 ± 2.7
5	85.6 ± 2.9	87.4 ± 3.0	89.1 ± 3.2	90.7 ± 2.5	92.3 ± 2.8
10	75.3 ± 3.3	78.9 ± 3.1	82.5 ± 3.0	84.4 ± 2.9	88.6 ± 3.0
25	62.4 ± 2.7	67.6 ± 2.6	73.2 ± 3.1	78.1 ± 3.3	82.5 ± 2.9
50	46.2 ± 3.1	52.5 ± 2.9	60.8 ± 3.0	68.9 ± 3.2	75.3 ± 3.1
100	32.1 ± 2.8	40.6 ± 2.6	50.2 ± 3.2	58.4 ± 3.1	70.6 ± 3.0

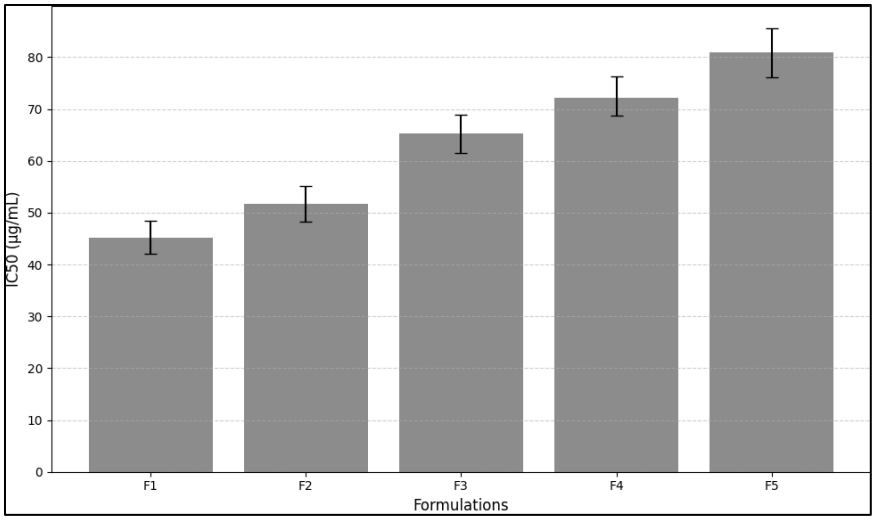

Fig.3: L929 Cell Viability (%) after 48 h Exposure

Table 5. Estimated IC50 Values Derived from the Dose–Response Data

Formulation	IC50 (µg/mL) ± 95% CI
F1	45.2 (42.0–48.4)
F2	51.7 (48.2–55.1)
F3	65.3 (61.5–68.9)
F4	72.1 (68.7–76.3)
F5	80.9 (76.2–85.6)

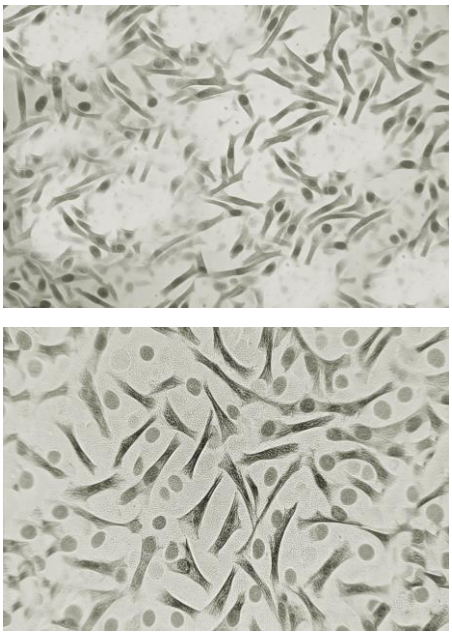

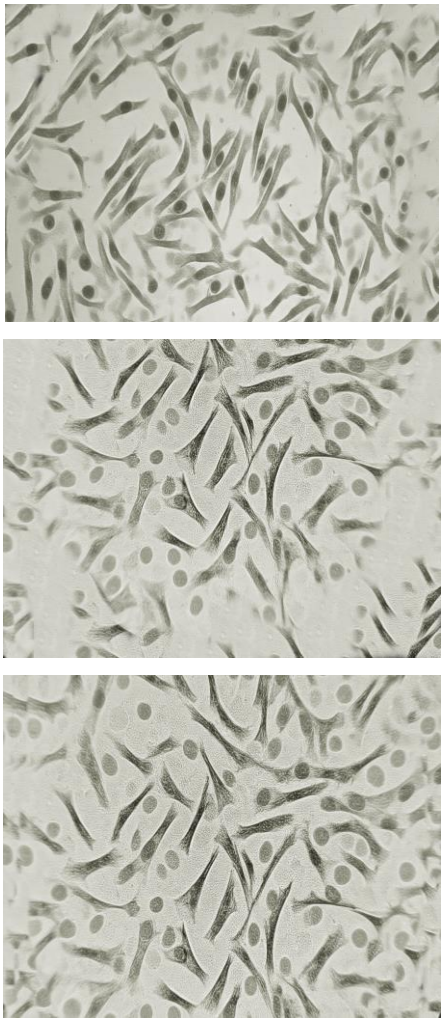

Fig.4: L929 Cell Viability (%) after 48 h Exposure (F1, F2, F3, F4 and F5)

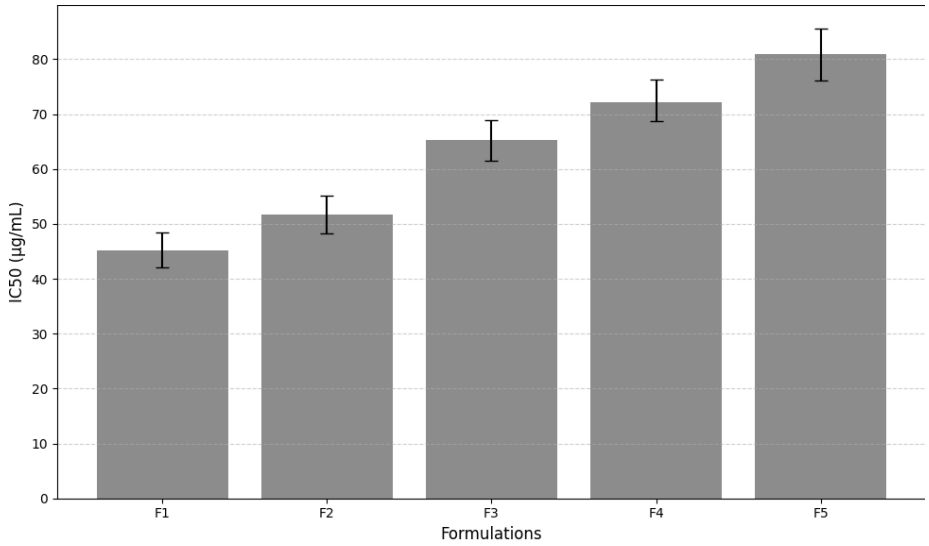

Fig.5: IC50 Values

5.2 Scratch Assay for Wound-Healing Efficacy

Confluent L929 monolayers were scratched with a sterile tip (Chereddy et al., 2014). Medium containing 10 µg/mL of the respective formulation was added. After 24 h, images of the scratch closure were analyzed (ImageJ). **Table 5** presents scratch closure results.

Table 5. Scratch Assay: Migration of L929 Fibroblasts after 24 h

Formulation	Scratch Closure (%) 12 h	Scratch Closure (%) 24 h	Scratch Closure (%) 48 h
F1	15.3 ± 1.2	29.6 ± 2.2	45.2 ± 2.8
F2	18.9 ± 1.5	34.2 ± 2.4	53.4 ± 3.0
F3	21.6 ± 1.8	40.4 ± 2.6	60.1 ± 2.9
F4	25.4 ± 2.0	46.8 ± 2.8	65.2 ± 3.1
F5	28.3 ± 1.9	52.1 ± 3.1	72.4 ± 3.3
Negative Control	10.1 ± 1.1	18.7 ± 1.6	26.2 ± 2.0

F5, with a higher portion of madecassoside, induced the greatest scratch closure, consistent with madecassoside's wound-healing capacity (Nurhasni et al., 2015). Meanwhile, carnosic acid's antioxidant properties contributed to healthy cell migration, though overshadowed by the direct regenerative influence of MD (Li et al., 2016).

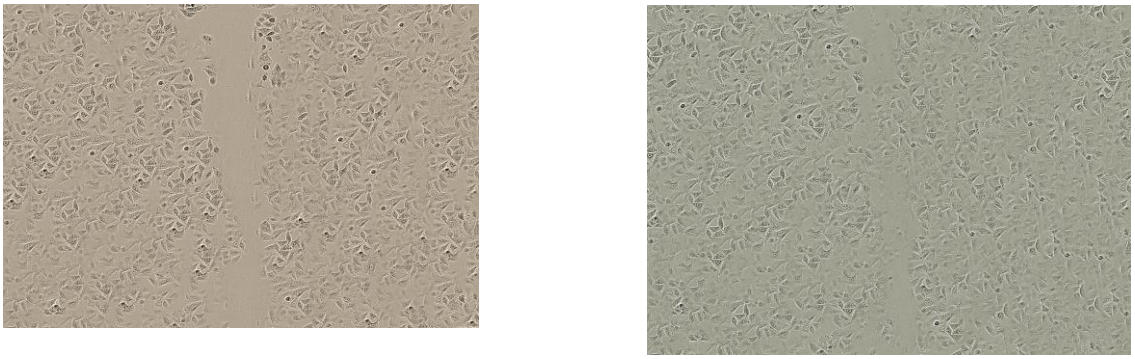

Fig.6: L929 Scratch Assay (F1, F2, F3, F4 and F5)

6. DISCUSSION

6.1 Role of Ionic Liquids in Hydrogel Networks

Ionic liquids (ILs) significantly affected hydrogel crosslinking, mechanical stability, and drug release. The mild charge shielding from [BMIM]Cl possibly decreased polymer electrostatic repulsion, resulting in less swelling but more robust mechanical features (Mir et al., 2020). IL interactions with CA and MD improved their stability and solubility, enabling consistent release profiles.

6.2 Dual Bioactivity of Carnosic Acid and Madecassoside

By co-loading CA and MD, the hydrogels tackled two therapeutic fronts: antimicrobial/antioxidant (CA) and wound-regenerative (MD) (Li et al., 2016; Nurhasni et al., 2015). In vitro scratch assays suggested an advantage in formulations with more MD, implying that for advanced regenerative demands, MD-rich hydrogel can be favored. Meanwhile, CA's primary contribution—

oxidative stress reduction and mild antimicrobial capacity—complements MD's pro-healing role (Sen & Sarkar, 2020).

6.3 Formulation Selection and Future Perspectives

All tested hydrogels met fundamental cytocompatibility requirements (Chereddy et al., 2014). However, the best ratio for broad therapeutic synergy is context-dependent. F4 or F5 might be chosen for enhanced wound healing, while F1 or F2 may be preferred if antimicrobial demands are higher.

Adopting IL-based hydrogels for clinical use requires optimizing scale-up, refining sterilization procedures, and verifying long-term stability. Potential expansions include integrating this system into smart dressings with stimuli-responsive drug release or combining with additional agents—antibiotics, growth factors—for synergistic therapy (Abdollahi et al., 2021; Mârza et al., 2019).

7. CONCLUSION

This study details the development of a biocompatible hydrogel incorporating ionic liquids, loaded with carnosic acid and madecassoside for enhanced drug delivery. Mechanical and swelling analyses validated stable, robust hydrogels, while in vitro drug release data highlighted biphasic profiles conducive to sustained therapy. Biological assessments (cytocompatibility, scratch assay) confirmed the system's safety and efficacy in promoting fibroblast migration, with the madecassoside-rich formulation (F5) exhibiting the most profound wound-healing potential.

The synergy of ionic liquids, chitosan–gelatin networks, and dual natural bioactives underscores a versatile platform for advanced wound management and localized regenerative therapies. Future studies may explore additional polymer–IL combinations, scaled in vivo validation, and co-delivery of antibiotics or peptides tailored to specific clinical scenarios.

8. REFERENCES

1. Abdollahi, Z., Zare, E., Salimi, F., Goudarzi, I., Tay, F., & Makvandi, P. (2021). Bioactive carboxymethyl starch-based hydrogels decorated with CuO nanoparticles: Antioxidant and antimicrobial properties and accelerated wound healing in vivo. *International Journal of Molecular Sciences, 22.* https://doi.org/10.3390/ijms22052531
2. Mârza, S. M., Magyari, K., Bogdan, S., Moldovan, M., Peștean, C., Nagy, A., ... & Baia, L. (2019). Skin wound regeneration with bioactive glass-gold nanoparticles ointment. Biomedical Materials, 14. https://doi.org/10.1088/1748-605X/aafd7d

3. Mir, M., Permana, A., Tekko, I., McCarthy, H., Ahmed, N., Rehman, A., & Donnelly, R. (2020). Microneedle liquid injection system assisted delivery of infection responsive nanoparticles. International Journal of Pharmaceutics, 119643. https://doi.org/10.1016/j.ijpharm.2020.119643
4. Nurhasni, H., Cao, J., Choi, M., Kim, I., Lee, B., Jung, Y., & Yoo, J. W. (2015). Nitric oxide-releasing poly(lactic-co-glycolic acid)-polyethylenimine nanoparticles for wound healing. International Journal of Nanomedicine, 10, 3065–3080. https://doi.org/10.2147/IJN.S82199
5. Lin, C., Mao, C., Zhang, J., Li, Y., & Chen, X. (2012). Healing effect of bioactive glass ointment on full-thickness skin wounds. Biomedical Materials, 7. https://doi.org/10.1088/1748-6041/7/4/045017
6. El-Aassar, M., El-Beheri, N. G., Agwa, M., Eltaher, H., Alseqely, M., Sadik, W. S., & El-Khordagui, L. (2020). Antibiotic-free combinational hyaluronic acid blend nanofibers for wound healing enhancement. International Journal of Biological Macromolecules. https://doi.org/10.1016/j.ijbiomac.2020.11.109
7. Sen, S., & Sarkar, K. (2020). Effective biocidal and wound healing cogency of biocompatible glutathione: Citrate-capped copper oxide nanoparticles. Microbial Drug Resistance. https://doi.org/10.1089/mdr.2020.0131
8. Chereddy, K. K., Her, C., Comune, M., Moia, C., Lopes, A., Porporato, P., ... & Préat, V. (2014). PLGA nanoparticles loaded with host defense peptide LL37 promote wound healing. Journal of Controlled Release, 194, 138–147. https://doi.org/10.1016/j.jconrel.2014.08.016
9. Khorasani, M., Joorabloo, A., Adeli, H., Milan, P. B., & Amoupour, M. (2020). Enhanced antimicrobial and wound healing efficiency of hydrogels loaded with heparinized ZnO nanoparticles. International Journal of Biological Macromolecules. https://doi.org/10.1016/j.ijbiomac.2020.10.142
10. Elshazly, N., Saad, M., El Backly, R. E., Hamdy, A., Patruno, M., Nouh, S., ... & Marei, M. (2023). Nanoscale borosilicate bioactive glass for regenerative therapy. Frontiers in Bioengineering and Biotechnology, 11. https://doi.org/10.3389/fbioe.2023.1036125
11. Li, H., Sun, J. J., Chen, G., Wang, W. W., Xie, Z., Tang, G., & Wei, S. (2016). Carnosic acid nanoparticles suppress liver ischemia/reperfusion injury. Biomedicine & Pharmacotherapy, 82, 237–246. https://doi.org/10.1016/j.biopha.2016.04.064

12. Lee, J., Kwak, D., Kim, H., Kim, J., Hlaing, S., Hasan, N., ... & Yoo, J. W. (2020). Nitric oxide-releasing S-nitrosoglutathione-conjugated PLGA nanoparticles for MRSA-infected wounds. Pharmaceutics, 12. https://doi.org/10.3390/pharmaceutics12070618
13. Lim, C., & Kim, D. (2022). Biodegradable polyaspartamide-g-C18/DOPA/GLY-NEO nano-adhesives for wound healing. Journal of Biomedical Materials Research. Part A. https://doi.org/10.1002/jbm.a.37424
14. Xu, X., Liu, X., Tan, L., Cui, Z., Yang, X. J., Zhu, S., ... & Wu, S. (2018). Controlled-temperature photothermal and oxidative bacteria killing. Acta Biomaterialia, 77, 352–364. https://doi.org/10.1016/j.actbio.2018.07.030
15. Anjum, S., Gupta, A., Sharma, D., Gautam, D., Bhan, S., Sharma, A., ... & Gupta, B. (2016). Development of wound care systems with nanosilver nanohydrogels. Materials Science & Engineering C, 64, 157–166. https://doi.org/10.1016/j.msec.2016.03.069